Open access • Journal Article • DOI:10.1139/CJP-2017-0241

Black hole shadows in fourth-order conformal Weyl gravity — Source link

Jonas Mureika, Gabriele U. Varieschi

Institutions: Loyola Marymount University

Published on: 14 Jun 2017 - Canadian Journal of Physics (NRC Research Press)

Topics: White hole

Canadian Science Publishing
NRC Research Press journals | Publishing Services

Canadian Journal of Physics
Revue canadienne de physique

Black hole shadows in fourth-order conformal Weyl gravity

Journal:	*Canadian Journal of Physics*
Manuscript ID	cjp-2017-0241.R1
Manuscript Type:	Article
Date Submitted by the Author:	04-May-2017
Complete List of Authors:	Mureika, Jonas; Loyola Marymount University Frank R Seaver College of Science and Engineering, Physics Varieschi, Gabriele; Loyola Marymount University Frank R Seaver College of Science and Engineering, Physics
Keyword:	modified gravity, conformal Weyl gravity, black hole shadows, astrophysical black holes, supermassive black holes
Is the invited manuscript for consideration in a Special Issue? :	N/A

Note: The following files were submitted by the author for peer review, but cannot be converted to PDF. You must view these files (e.g. movies) online.

BHshadows_v7.bbl

Black hole shadows in fourth-order conformal Weyl gravity

Jonas R. Mureika* and Gabriele U. Varieschi†

Department of Physics, Loyola Marymount University - Los Angeles, CA 90045, USA

Abstract

We calculate the characteristics of the "black hole shadow" for a rotating, neutral black hole in fourth-order conformal Weyl gravity. It is shown that the morphology is not significantly affected by the underlying framework, except for very large masses. Conformal gravity black hole shadows would also significantly differ from their general relativistic counterparts if the values of the main conformal gravity parameters, γ and κ, were increased by several orders of magnitude. Such increased values for γ and κ are currently ruled out by gravitational phenomenology. Therefore, it is unlikely that these differences in black hole shadows will be detected in future observations, carried out by the Event Horizon Telescope or others such experiments.

PACS numbers: 04.50.Kd; 04.20.Jb; 04.70.-s; 97.60.Lf

Keywords: modified gravity, conformal gravity, astrophysical black holes.

* Email: jmureika@lmu.edu
† Email: gvarieschi@lmu.edu

Contents

I. INTRODUCTION

Immediately following the centenary of Einstein's general relativity (GR), we have been witness to a major test of the theory's foundational predictions. Two separate detections by LIGO of gravitational waves from binary black hole (BH) mergers [1–3] have provided incontrovertible experimental evidence of this long-predicted feature of GR. A second test – the imaging of a black hole's "shadow"/photosphere, and by proxy its event horizon – is looming near. Pioneered by the Event Horizon Telescope (EHT) and BlackHoleCam consortia [4, 5], it will involve targeting the putative supermassive black hole Sagittarius A* (Sgr A*) at the center of the Milky Way [6], as well as active galactic nuclei [7], and it is anticipated that this will provide a crucial test of GR against competing theories by allowing precision measurements of the horizon size [8].

This and other morphological characteristics of the Sgr A* shadow will allow for precision measurement of the object's mass, but in principle can also be used to probe the curvature, and thus the underlying gravitational theory. Since astrophysical black holes are generally expected to be rotating and neutral, a baseline standard for general relativity can be extracted from an analysis of the Kerr solution [9, 10]. Given this fact, it is possible that such

data will also be sensitive to modifications of the underlying gravitational theory.

To date, a number of studies have addressed aspects of the shadow morphology associated with alternate theories and extensions to general relativity, and the literature is growing increasingly comprehensive. Select approaches include analyzing the shadow characteristics of Kerr black holes with scalar hair [11], a five-dimensional Myers-Perry black hole [12], distorted Schwarzschild [13] and Kerr black holes [14], as well as the possibility of observing double images from a single black hole [15]. Additional shadow traits in other extensions and alternatives to general relativity include noncommutative gravity inspired black holes [16], Modified Gravity [17], $f(r)$ gravity [18], a rotating Einstein-Born-Infeld black hole [19], regular black holes [20], and rotating non-singular black holes [21].

Furthermore, the EHT and related experiments could provide a novel test of Hawking radiation and string inspired theories through near horizon effects. Such phenomena will implicitly depend on the transfer of information across the horizon, and could effectively address the information paradox. One such example concerns the phenomenological impact of couplings between a black hole's internal states and those immediately outside the horizon, which manifest themselves as (quantum) spacetime fluctuations [22–26]. Although appearing at low energy scales, these fluctuations can be significant in magnitude, and can deflect near-horizon geodesics that span distances on the order of the black hole's radius. That is, the EHT can be used as an effective test of the information paradox, and a coherent analysis of near-horizon physics may open a window to quantum gravity.

The associated conclusions are mixed as to whether or not the modification of choice will have any measurable impact on the shadow within the limit of the experimental sensitivity. These range from shadow sizes both smaller and larger than the general relativistic predictions, as well as morphological discrepancies (*e.g.* asymmetric shapes). As illustrative examples, the Einstein-Born-Infeld shadow considered in [19] was found to be smaller than that of a Reissner-Nordström black hole. Other models such as the Kerr black hole with scalar hair predict shadows of distinguishable shape from those in general relativity [14]. Differentiability of shadow characteristic by the EHT between Randall-Sundrum and Einstein-Gauss-Bonnet black holes have also been considered [8]. Perhaps the most compelling result is that for the Modified Gravity black hole [17], which predicts a shadow radius bigger than that of the standard Kerr solution, depending on the (non-universal) size of the Modified Gravity parameter α.

In the following paper, we address aspects of the black hole shadow in a fourth-order conformal Weyl gravity framework. Conformal gravity – or CG for short – is a natural extension of Einstein's general relativity, originally introduced by H. Weyl [27], revisited by P. Mannheim and others [28–34], and even considered by G. 't Hooft [35–38] as a possible key towards a complete understanding of physics at the Planck scale.

Conformal gravity naturally addresses and solves several cosmological and astrophysical problems [39], such as the cosmological constant problem [40, 41], zero-point energy and quantum gravity problems [42], the fitting of galactic rotation curves [43] and accelerating universe supernovae data [30], without any dark matter or dark energy.

It was recently noted by Maldacena that there is a holographic connection of CG to Einstein gravity (EG) [44], in the sense that CG reduces to EG for certain boundary conditions. Furthermore, it was shown by Grumiller, Irakleidou, Lovrekovic, and McNees that by generalizing the Starobinski boundary conditions in [44], the aforementioned CG solutions of Mannheim *et al.* can reproduce the solutions of Mannheim and Kazanas [28] and Riegert [45] with finite holographic response functions.

Although fourth-order gravity theories have long been thought to possess ghosts when quantized, it has recently been suggested that CG may be ghost-free [46–48] and unitary [49, 50]. These analyses rely on a heuristic comparison of CG to the Pais-Uhlenbech oscillator [51], but do not provide a definite treatment of CG.

Since the effects of CG do not manifest themselves at short distances [52], we seek in this paper to understand what impact the large-scale deviations will have on the morphology of a supermassive black hole shadow. Section II provides a short review of the general CG formalism. In Section III, we start with a brief review of the CG Kerr metric for a rotating black hole and then we describe the procedure used to obtain the BH shadows in conformal gravity. In Section IV, we consider specific cases of BH shadows, comparing GR and CG results; finally, in Section V, we present our conclusions.

II. CONFORMAL GRAVITY: A BRIEF REVIEW

Conformal gravity is based on the Weyl action:

$$I_W = -\alpha_g \int d^4x \, (-g)^{1/2} \, C_{\lambda\mu\nu\kappa} \, C^{\lambda\mu\nu\kappa}, \tag{1}$$

where $g \equiv \det(g_{\mu\nu})$, $C_{\lambda\mu\nu\kappa}$ is the conformal (or Weyl) tensor, and α_g is the CG coupling constant. I_W is the unique general coordinate scalar action that is invariant under local conformal transformations: $g_{\mu\nu}(x) \to e^{2\alpha(x)} g_{\mu\nu}(x) = \Omega^2(x) g_{\mu\nu}(x)$. The factor $\Omega(x) = e^{\alpha(x)}$ determines the amount of local stretching of the geometry, hence the name conformal for a theory invariant under all local stretchings of the space-time (see [31] and references therein for more details).

This conformally invariant generalization of GR was found to be a fourth-order theory, as opposed to the standard second-order General Relativity, since the field equations contained derivatives up to the fourth order of the metric with respect to the space-time coordinates [53]. The fourth-order CG field equations, $4\alpha_g W_{\mu\nu} = T_{\mu\nu}$ (where $W_{\mu\nu}$ is the Bach tensor—see [30, 31] for full details) were studied in 1984 by Riegert [45], who obtained the most general, spherically symmetric, static electrovacuum solution. The explicit form of this solution, for the practical case of a static, spherically symmetric source in CG, i.e., the fourth-order analogue of the Schwarzschild exterior solution in GR, was then derived by Mannheim and Kazanas in 1989 [28, 29]. This latter solution, in the case $T_{\mu\nu} = 0$ (exterior solution), is described by the metric

$$ds^2 = -B(r)\ c^2 dt^2 + \frac{dr^2}{B(r)} + r^2(d\theta^2 + \sin^2\theta\ d\phi^2), \tag{2}$$

with

$$B(r) = 1 - 3\beta\gamma - \frac{\beta(2 - 3\beta\gamma)}{r} + \gamma r - \kappa r^2. \tag{3}$$

The three integration constants in the last equation are as follows: β (cm) can be considered the CG equivalent of the geometrized mass $\frac{GM}{c^2}$, where M is the mass of the (spherically symmetric) source and G is the universal gravitational constant; two additional parameters, γ (cm^{-1}) and κ (cm^{-2}), are required by CG, while the standard Schwarzschild solution is recovered for $\gamma, \kappa \to 0$ in the equations above. The quadratic term $-\kappa r^2$ indicates a background De Sitter spacetime, which is important only over cosmological distances, since κ has a very small value. Similarly, γ measures the departure from the Schwarzschild metric at smaller distances, since the γr term becomes significant over galactic distance scales.

The values of the CG parameters were first determined by Mannheim [30]:

$$\gamma = 3.06 \times 10^{-30}\,\mathrm{cm}^{-1},\ \kappa = 9.54 \times 10^{-54}\,\mathrm{cm}^{-2} \tag{4}$$

and were also evaluated by one of us [31, 32] with a different approach, obtaining values

which differ by a few orders of magnitude from those above:

$$\gamma = 1.94 \times 10^{-28}\,\mathrm{cm}^{-1},\ \kappa = 6.42 \times 10^{-48}\,\mathrm{cm}^{-2}\,. \tag{5}$$

Mannheim et al. [30, 43, 54–58] used the CG solutions in Eqs. (2)-(3) to perform extensive data fitting of galactic rotation curves without any dark matter contribution, using the values of γ and κ as in Eq. (4). Although the values of these CG parameters are very small, the linear and quadratic terms in Eq. (3) become significant over galactic and/or cosmological distances.

There has been some debate as to nature of CG's short distance (GR) and weak field (Newtonian) limits. It was originally shown by Mannheim and Kazanas that fourth-order conformal gravity respectively recovers both frameworks in the appropriate limit [28, 59]. Although an objection was raised by Flanagan in [60] that this might be spoiled by the presence of a macroscopic scalar field that contributes to the stress-energy tensor, it was later shown that this would still not influence the Schwarzschild limit [52]. An additional criticism was levelled by Yoon in [61] that the potential does not possess a Newtonian limit for classical point particles. It was shown very recently by Mannheim, however, that this assumption violates the conformal invariance of the theory and is an incorrect conclusion [62].

III. ROTATING BLACK HOLES IN CONFORMAL GRAVITY

The standard GR Kerr metric is [63] ($c = G = 1$ in the following):

$$ds^2 = -\rho^2\frac{\Delta}{\Sigma^2}\,dt^2 + \frac{\Sigma^2}{\rho^2}\left[d\phi - \frac{2aMr}{\Sigma^2}dt\right]^2 \sin^2\theta\ + \frac{\rho^2}{\Delta}\,dr^2 + \rho^2 d\theta^2, \tag{6}$$

with

$$\rho^2 \equiv r^2 + a^2\cos^2\theta\ ;\ \Delta \equiv r^2 - 2Mr + a^2\ ;\ \Sigma^2 \equiv \left(r^2+a^2\right)^2 - a^2\Delta\sin^2\theta. \tag{7}$$

In these equations a is the angular momentum parameter ($a = J/M$) and M is the geometrized mass.

A. Kerr metric in CG

The CG fourth-order Kerr metric, originally introduced by Mannheim and Kazanas in 1991 [64], can also be written in a similar way[1] [33]:

$$ds^2 = -\rho^2 \frac{\widetilde{\Delta}_r \, \widetilde{\Delta}_\theta}{\widetilde{\Sigma}^2} \, dt^2 + \frac{\widetilde{\Sigma}^2}{\rho^2} \left[d\phi + \frac{\widetilde{\Delta}_r - (r^2+a^2)\, \widetilde{\Delta}_\theta}{\widetilde{\Sigma}^2} a \, dt \right]^2 \sin^2\theta \; + \frac{\rho^2}{\widetilde{\Delta}_r} \, dr^2 + \frac{\rho^2}{\widetilde{\Delta}_\theta} d\theta^2, \quad (8)$$

with extended definitions for the CG auxiliary quantities and functions:

$$\widetilde{M} \equiv M \left(1 - \frac{3}{2} \, M\gamma \right) \; ; \; \widetilde{\Delta}_r \equiv r^2 - 2\widetilde{M} r + a^2 - k r^4; \quad (9)$$
$$\widetilde{\Delta}_\theta \equiv 1 - k a^2 \cos^2\theta \cot^2\theta \; ; \; \widetilde{\Sigma}^2 \equiv \widetilde{\Delta}_\theta \left(r^2 + a^2 \right)^2 - a^2 \widetilde{\Delta}_r \sin^2\theta.$$

We note that the CG fourth-order Kerr metric is conformal to the standard second-order Kerr-de Sitter metric, as originally proven by Mannheim and Kazanas [64].

The constant k is related to both parameters γ and κ of conformal gravity:

$$k = \kappa + \frac{\gamma^2 (1 - M\gamma)}{(2 - 3M\gamma)^2}. \quad (10)$$

However, these parameters γ and κ are very small; current estimates give [30, 31, 34]:

$$\gamma \sim 10^{-30} - 10^{-28} \, \mathrm{cm}^{-1}, \quad (11)$$
$$\kappa \sim 10^{-54} - 10^{-48} \, \mathrm{cm}^{-2},$$

as shown also in Eqs. (4)-(5). It is easy to check that for $\gamma, \kappa \to 0$ the Kerr CG metric reduces to the standard Kerr GR metric.

Dimensionless parameters to be used in the analysis of BH shadows are defined as:

$$a_* = \frac{a}{M}; \;\; \widetilde{a}_* = \frac{a}{\widetilde{M}}; \quad (12)$$
$$\gamma_* = \gamma M \sim 10^{-24} - 10^{-14};$$
$$k_* = k\widetilde{M}^2 \sim 10^{-42} - 10^{-20}.$$

[1] In general, CG quantities will be denoted by a tilde (˜) superscript.

The condition for the existence of the GR event horizon is $|a_*| \leq 1$, obtained from the equation $\Delta = r^2 - 2Mr + a^2 = 0$; in CG the equivalent equation $\widetilde{\Delta}_r = r^2 - 2\widetilde{M}r + a^2 - kr^4 = 0$ will be solved numerically, for the cases of interest in Sect. IV.

The ranges for γ_* and k_* in Eq. (12) were estimated as follows: we assume BH masses in the range $\widetilde{M} \sim M \sim (10 - 10^9)\, M_\odot \sim 10^6 - 10^{14}\,\mathrm{cm}$, since BH masses range [9] from $M \sim 10 M_\odot$ (dark compact objects) to $M \sim 10^9 M_\odot$ (heaviest super-massive BH), with $M_\odot \sim 10^5\,\mathrm{cm}$. These numbers are then combined with the ranges for γ and κ in Eq. (11) and with $k \approx \kappa$, due to Eq. (10).

Following [9], [63], and [33] the radial equation of motion for photons is:

$$\dot{r}^2 = \left(\frac{dr}{d\tau}\right)^2 = \left\{ \begin{array}{l} \frac{\widetilde{R}(r)}{\rho^4} = \frac{\widetilde{\Delta}_r{}^2}{\rho^4} p_r^2 \ ; \ \text{4th-order CG} \\ \frac{R(r)}{\rho^4} = \frac{\Delta^2}{\rho^4} p_r^2 \ ; \ \text{2nd-order GR} \end{array} \right\}, \tag{13}$$

with τ being an affine parameter, and (for photons)

$$\begin{aligned} \widetilde{R}(r) &\equiv \left[\left(r^2 + a^2\right) E - a L_z\right]^2 - \widetilde{\Delta}_r [\widetilde{\mathcal{Q}} + (L_z - aE)^2] \\ &= [E^2 + k((aE - L_z)^2 + \widetilde{\mathcal{Q}})] r^4 + (a^2 E^2 - L_z^2 - \widetilde{\mathcal{Q}}) r^2 + 2\widetilde{M}[(aE - L_z)^2 + \widetilde{\mathcal{Q}}] r - a^2 \widetilde{\mathcal{Q}} \\ R(r) &\equiv \left[\left(r^2 + a^2\right) E - a L_z\right]^2 - \Delta [\mathcal{Q} + (L_z - aE)^2] \\ &= E^2 r^4 + (a^2 E^2 - L_z^2 - \mathcal{Q}) r^2 + 2M[(aE - L_z)^2 + \mathcal{Q}] r - a^2 \mathcal{Q}, \end{aligned} \tag{14}$$

respectively, in the CG and GR cases. E and L_z are interpreted respectively as energy per unit mass and angular momentum—in the axial direction—per unit mass, while Carter's constant (for photons) is also different in the two cases:

$$\begin{aligned} \widetilde{\mathcal{Q}} &= \widetilde{\Delta}_\theta p_\theta^2 + \frac{(aE \sin\theta - L_z \csc\theta)^2}{\widetilde{\Delta}_\theta} - (L_z - aE)^2 \\ \mathcal{Q} &= p_\theta^2 + (aE \sin\theta - L_z \csc\theta)^2 - (L_z - aE)^2 \\ &= p_\theta^2 + \cos^2\theta \left(\frac{L_z^2}{\sin^2\theta} - a^2 E^2\right). \end{aligned} \tag{15}$$

We note that Carter's constant in CG ($\widetilde{\mathcal{Q}}$) cannot be written in a form similar to the one for $\mathcal{Q}$ in the last line of the previous equation.

It is customary to minimize the parameters by setting:

$$\xi = \widetilde{\xi} = L_z/E \ ; \ \eta = \mathcal{Q}/E^2 \ ; \ \widetilde{\eta} = \widetilde{\mathcal{Q}}/E^2 \tag{16}$$

and rewrite Eq. (14) in terms of modified functions (rescaled functions, dividing by E^2): $R(r) = R(r)/E^2$ and $\widetilde{R}(r) = \widetilde{R}(r)/E^2$. These modified radial functions (for photons) can be written explicitly as:

$$\widetilde{R}(r) = [1 + k(\widetilde{\eta} + (\widetilde{\xi} - a)^2)]r^4 + (a^2 - \widetilde{\xi}^2 - \widetilde{\eta})r^2 + 2\widetilde{M}[\widetilde{\eta} + (\widetilde{\xi} - a)^2]r - a^2\widetilde{\eta} \tag{17}$$
$$R(r) = r^4 + (a^2 - \xi^2 - \eta)r^2 + 2M[\eta + (\xi - a)^2]r - a^2\eta$$

where, as usual, the CG case reduces to the GR case for $\gamma, \kappa \to 0$.

Similarly, rescaled angular functions $\Theta(\theta) = \Theta(\theta)/E^2$ and $\widetilde{\Theta}(\theta) = \widetilde{\Theta}(\theta)/E^2$ are also introduced (see [63] and [33] for details):

$$\widetilde{\Theta}(\theta) = \widetilde{\Delta}_\theta\widetilde{\eta} + a^2\cos^2\theta + (\widetilde{\Delta}_\theta - 1)(\widetilde{\xi} - a)^2 - \widetilde{\xi}^2\cot^2\theta \tag{18}$$
$$\Theta(\theta) = \eta + a^2\cos^2\theta - \xi^2\cot^2\theta$$

B. Black hole shadows in CG

BH shadows are related to unstable circular photon orbits. These are obtained by setting $\widetilde{R}(r) = \frac{\partial\widetilde{R}}{\partial r} = 0$ and $R(r) = \frac{\partial R}{\partial r} = 0$ for our two cases. Explicitly:

$$[1 + k(\widetilde{\eta}_c + (\widetilde{\xi}_c - a)^2)]r^4 + (a^2 - \widetilde{\xi}_c^2 - \widetilde{\eta}_c)r^2 + 2\widetilde{M}[\widetilde{\eta}_c + (\widetilde{\xi}_c - a)^2]r - a^2\widetilde{\eta}_c = 0 \tag{19}$$
$$4[1 + k(\widetilde{\eta}_c + (\widetilde{\xi}_c - a)^2)]r^3 + 2(a^2 - \widetilde{\xi}_c^2 - \widetilde{\eta}_c)r + 2\widetilde{M}[\widetilde{\eta}_c + (\widetilde{\xi}_c - a)^2] = 0$$

and

$$r^4 + (a^2 - \xi_c^2 - \eta_c)r^2 + 2M[\eta_c + (\xi_c - a)^2]r - a^2\eta_c = 0 \tag{20}$$
$$4r^3 + 2(a^2 - \xi_c^2 - \eta_c)r + 2M[\eta_c + (\xi_c - a)^2] = 0$$

where $(\widetilde{\xi}_c, \widetilde{\eta}_c)$ and (ξ_c, η_c) represent the critical loci, i.e., the set of unstable circular photon orbits in the two cases.

Following the procedure outlined in [63] or in [65], we can solve these equations for the CG case and obtain:

$$\widetilde{\xi}_c = \frac{[\widetilde{M}(r^2-a^2) - r(r^2 - 2\widetilde{M}r + a^2) - 2a^2kr^3]}{a(r-\widetilde{M}-2kr^3)} = \frac{[\widetilde{M}(r^2-a^2) - r\widetilde{\Delta}_r - kr^3(r^2+2a^2)]}{a(r-\widetilde{M}-2kr^3)}$$
$$\widetilde{\eta}_c = \frac{r^3[4a^2\widetilde{M} - r(r-3\widetilde{M})^2 - 4a^2kr^3]}{a^2(r-\widetilde{M}-2kr^3)^2} = \frac{r^3[4\widetilde{M}\widetilde{\Delta}_r + 4kr^3(\widetilde{M}r - a^2) - r(r-\widetilde{M})^2]}{a^2(r-\widetilde{M}-2kr^3)^2}, \tag{21}$$

similar to the second-order solutions:

$$\xi_c = \frac{[M(r^2-a^2) - r(r^2-2Mr+a^2)]}{a(r-M)} = \frac{[M(r^2-a^2) - r\Delta]}{a(r-M)}$$
$$\eta_c = \frac{r^3[4a^2M - r(r-3M)^2]}{a^2(r-M)^2} = \frac{r^3[4M\Delta - r(r-M)^2]}{a^2(r-M)^2}. \tag{22}$$

Since plots of BH shadows are usually done with coordinates expressed in units of mass, it is more practical to rewrite the previous solutions in Eqs. (21) and (22) in terms of dimensionless quantities (capital Xi and capital Eta) as follows:

$$\widetilde{\Xi}_c = \frac{\widetilde{\xi}_c}{\widetilde{M}} = \frac{[(\widetilde{z}^2 - \widetilde{a}_*^2) - \widetilde{z}(\widetilde{z}^2 - 2\widetilde{z} + \widetilde{a}_*^2) - 2\widetilde{a}_*^2k_*\widetilde{z}^3]}{\widetilde{a}_*(\widetilde{z} - 1 - 2k_*\widetilde{z}^3)}$$
$$\widetilde{H}_c = \frac{\widetilde{\eta}_c}{\widetilde{M}^2} = \frac{\widetilde{z}^3[4\widetilde{a}_*^2 - \widetilde{z}(\widetilde{z}-3)^2 - 4\widetilde{a}_*^2k_*\widetilde{z}^3]}{\widetilde{a}_*^2(\widetilde{z} - 1 - 2k_*\widetilde{z}^3)^2}, \tag{23}$$

and

$$\Xi_c = \frac{\xi_c}{M} = \frac{[(z^2 - a_*^2) - z(z^2 - 2z + a_*^2)]}{a_*(z-1)}$$
$$H_c = \frac{\eta_c}{M^2} = \frac{z^3[4a_*^2 - z(z-3)^2]}{a_*^2(z-1)^2}. \tag{24}$$

In the previous two equations, we used the dimensionless radial variables $z = r/M$ and $\widetilde{z} = r/\widetilde{M}$, and also the dimensionless parameters from Eq. (12).

The last step in the procedure for plotting BH shadows is to consider the celestial coordinates x and y of the image, as seen by an observer at infinity. The standard GR procedure [63, 65], considers the tetrad components of the four momentum as:

$$
\begin{aligned}
p^{(t)} &= e^{-\nu}(E - \omega L_z) = \frac{\Sigma}{\rho\sqrt{\Delta}}\left(E - \frac{2aMr}{\Sigma^2}L_z\right) \\
p^{(r)} &= -e^{-\mu_2}p_r = \frac{\sqrt{\Delta}}{\rho}\frac{\sqrt{R(r)}}{\Delta} = \frac{1}{\rho}\sqrt{\frac{R(r)}{\Delta}} \\
p^{(\theta)} &= -e^{-\mu_3}p_\theta = \frac{1}{\rho}\sqrt{\Theta(\theta)} = \frac{1}{\rho}\sqrt{\left(\eta + a^2\cos^2\theta - \xi^2\cot^2\theta\right)E^2} \\
p^{(\phi)} &= e^{-\psi}L_z = \frac{\rho}{\sin\theta\ \Sigma}L_z,
\end{aligned}
\tag{25}
$$

where ν, ω, μ_2, μ_3, and ψ are functions of r and θ, which can be expressed in terms of all the other functions used previously.

The celestial coordinates x and y of the image are then computed in terms of ξ, η, and of the angular coordinate of the observer at infinity, $\theta \to i$:

$$
\begin{aligned}
x &= \left(\frac{rp^{(\phi)}}{p^{(t)}}\right)_{r\to\infty} = \frac{\xi}{\sin i} \\
y &= \left(\frac{rp^{(\theta)}}{p^{(t)}}\right)_{r\to\infty} = \pm\left(\eta + a^2\cos^2 i - \xi^2\cot^2 i\right)^{1/2},
\end{aligned}
\tag{26}
$$

where the previous equation is obtained by using the quantities in Eq. (25) and taking limits for $r \to \infty$.

Rescaling also the celestial coordinates into dimensionless ones, $X = x/M$ and $Y = y/M$, and combining together Eqs. (24) and (26), yields the parametric form of the critical locus in dimensionless coordinates:

$$
\begin{aligned}
X &= \frac{x}{M} = \frac{\xi_c/M}{\sin i} = \frac{\Xi_c}{\sin i} = \frac{1}{\sin i}\frac{[(z^2 - a_*^2) - z(z^2 - 2z + a_*^2)]}{a_*(z-1)} \\
Y &= \frac{y}{M} = \pm\left(\frac{\eta_c}{M^2} + \frac{a^2}{M^2}\cos^2 i - \frac{\xi_c^2}{M^2}\cot^2 i\right)^{1/2} = \pm\left(H_c + a_*^2\cos^2 i - \Xi_c^2\cot^2 i\right)^{1/2} \\
&= \pm\left\{\frac{z^3[4a_*^2 - z(z-3)^2]}{a_*^2(z-1)^2} + a_*^2\cos^2 i - \left[\frac{(z^2 - a_*^2) - z(z^2 - 2z + a_*^2)}{a_*(z-1)}\right]^2\cot^2 i\right\}^{1/2}.
\end{aligned}
\tag{27}
$$

This locus can be plotted for values of the parameter $z \gtrsim 1 + \sqrt{1 - a_*^2}$ obtaining the standard GR shadows that will be shown in Sect. IV.

The same procedure can be repeated in CG; the equivalent of Eq. (25) in CG is:

$$p^{(t)} = e^{-\nu}(E - \omega L_z) = \frac{\widetilde{\Sigma}}{\rho\sqrt{\widetilde{\Delta}_r\widetilde{\Delta}_\theta}}\left(E - \frac{-\widetilde{\Delta}_r + (r^2+a^2)\widetilde{\Delta}_\theta}{\widetilde{\Sigma}^2}aL_z\right) \tag{28}$$

$$p^{(r)} = -e^{-\mu_2}p_r = \frac{\sqrt{\widetilde{\Delta}_r}}{\rho}\frac{\sqrt{\widetilde{R}(r)}}{\widetilde{\Delta}_r} = \frac{1}{\rho}\sqrt{\frac{\widetilde{R}(r)}{\widetilde{\Delta}_r}}$$

$$p^{(\theta)} = -e^{-\mu_3}p_\theta = \frac{\sqrt{\widetilde{\Delta}_\theta}}{\rho}\frac{\sqrt{\widetilde{\Theta}(\theta)}}{\widetilde{\Delta}_\theta} = \frac{1}{\rho}\sqrt{\frac{\widetilde{\Delta}_\theta\widetilde{\eta} + a^2\cos^2\theta + (\widetilde{\Delta}_\theta - 1)(\widetilde{\xi}-a)^2 - \widetilde{\xi}^2\cot^2\theta}{\widetilde{\Delta}_\theta}E^2}$$

$$p^{(\phi)} = e^{-\psi}L_z = \frac{\rho}{\sin\theta\,\widetilde{\Sigma}}L_z.$$

The celestial coordinates $\widetilde{x}$ and $\widetilde{y}$ of the image, as a function of $\widetilde{\xi}$, $\widetilde{\eta}$, and of the angular coordinate of the observer at infinity, $\theta \to i$, are obtained by considering the leading terms for large r ($r \gg a$ and $r \gg \widetilde{M}$). CG terms proportional to ka are neglected, due to the small value of k, but terms such as $(1-kr^2)^{1/2}$ and $(1-ka^2\cos^2 i\cot^2 i)^{1/2}$ are included, as possible CG corrections:

$$\widetilde{x} = \left(\frac{rp^{(\phi)}}{p^{(t)}}\right)_{r\gg a,\widetilde{M}} = \frac{\widetilde{\xi}}{\sin i}\frac{(1-kr^2)^{1/2}}{(1-ka^2\cos^2 i\cot^2 i)^{1/2}} \tag{29}$$

$$\widetilde{y} = \left(\frac{rp^{(\theta)}}{p^{(t)}}\right)_{r\gg a,\widetilde{M}} = \pm\left[\left(1-ka^2\cos^2 i\cot^2 i\right)\widetilde{\eta} + a^2\cos^2 i - ka^2\cos^2 i\cot^2 i(\widetilde{\xi}-a)^2 - \widetilde{\xi}^2\cot^2 i\right]^{1/2}$$
$$\times\frac{(1-kr^2)^{1/2}}{(1-ka^2\cos^2 i\cot^2 i)^{1/2}}.$$

Due to the presence of the $(1-kr^2)^{1/2}$ terms, the CG expressions for $\widetilde{x}$ and $\widetilde{y}$ are divergent for $r\to\infty$, but they can be considered as valid approximations for $r < \sqrt{k^{-1}} \sim 10^{24} - 10^{27}$ cm.

The dimensionless celestial coordinates $\widetilde{X} = \widetilde{x}/\widetilde{M}$ and $\widetilde{Y} = \widetilde{y}/\widetilde{M}$ in CG become:

$$\widetilde{X} = \frac{\widetilde{x}}{\widetilde{M}} = \frac{\widetilde{\Xi}_c}{\sin i}\frac{(1-k_*\widetilde{z}^2)^{1/2}}{(1-k_*\widetilde{a}_*^2\cos^2 i\cot^2 i)^{1/2}} \tag{30}$$

$$\widetilde{Y} = \frac{\widetilde{y}}{\widetilde{M}} = \pm\left[(1-k_*\widetilde{a}_*^2\cos^2 i\cot^2 i)\widetilde{H}_c + \widetilde{a}_*^2\cos^2 i - k_*\widetilde{a}_*^2\cos^2 i\cot^2 i\,(\widetilde{\Xi}_c - \widetilde{a}_*)^2 - \widetilde{\Xi}_c^2\cot^2 i\right]^{1/2}$$
$$\times\frac{(1-k_*\widetilde{z}^2)^{1/2}}{(1-k_*\widetilde{a}_*^2\cos^2 i\cot^2 i)^{1/2}},$$

which correctly reduce to the GR dimensionless coordinates in Eq. (27) for $k_*\to 0$ and $\widetilde{M}\to M$. In the next section, we will use the GR and CG expressions for the dimensionless

celestial coordinates (equations (27) and (30), respectively), in order to plot the black hole shadows in these two cases.

Since the GR and CG shadow plots will be directly compared with each other, we will need all coordinates to be expressed in terms of the standard mass M, i.e., the $\widetilde{X}$ and $\widetilde{Y}$ coordinates need to be rescaled by a common factor $(1-\frac{3}{2}M\gamma) = (1-\frac{3}{2}\gamma_*)$, in view of Eqs. (9) and (12). Explicitly:

$$X_{(CG)} = \frac{\widetilde{x}}{M} = \widetilde{X}\frac{\widetilde{M}}{M} = \widetilde{X}\left(1-\frac{3}{2}\gamma_*\right) \tag{31}$$
$$Y_{(CG)} = \frac{\widetilde{y}}{M} = \widetilde{Y}\frac{\widetilde{M}}{M} = \widetilde{Y}\left(1-\frac{3}{2}\gamma_*\right),$$

where $X_{(CG)}$ and $Y_{(CG)}$ indicate these rescaled CG coordinates, to be compared with the rescaled GR coordinates in Eq. (27).

IV. SPECIFIC CASES OF BH SHADOWS

In this section, we will plot the CG black hole shadows, following Eqs. (30)-(31), and compare them with the GR shadows, following Eq. (27), for several cases of interest.

As our first example, we consider the case of Sagittarius A*, the supermassive black hole at the center of our galaxy, already mentioned in Sect. I. Its mass and distance are estimated as follows:

$$M = \left\{ \begin{array}{c} (4.31 \pm 0.38) \times 10^6 M_\odot = (6.36 \pm 0.56) \times 10^{11}\,\text{cm} \;\; [66] \\ (4.1 \pm 0.6) \times 10^6 M_\odot = (6.1 \pm 0.9) \times 10^{11}\,\text{cm} \;\; [67] \\ (4.02 \pm 0.16) \times 10^6 M_\odot = (5.94 \pm 0.24) \times 10^{11}\,\text{cm} \;\; [68] \end{array} \right\} \tag{32}$$
$$r = \left\{ \begin{array}{c} (7,940 \pm 420)\; pc = (2.45 \pm 0.13) \times 10^{22}\,\text{cm} \;\; [69] \\ (7,860 \pm 140)\; pc = (2.425 \pm 0.043) \times 10^{22}\,\text{cm} \;\; [68] \end{array} \right\}$$

In Fig. 1 we plot the GR and CG shadows of Sgr A*, for different values of the angular coordinate i and of the dimensionless angular momentum parameter a_*. The GR shadow plots are independent of the black hole mass, since they use the dimensionless coordinates X and Y from Eq. (27). The CG plots use instead the rescaled dimensionless coordinates

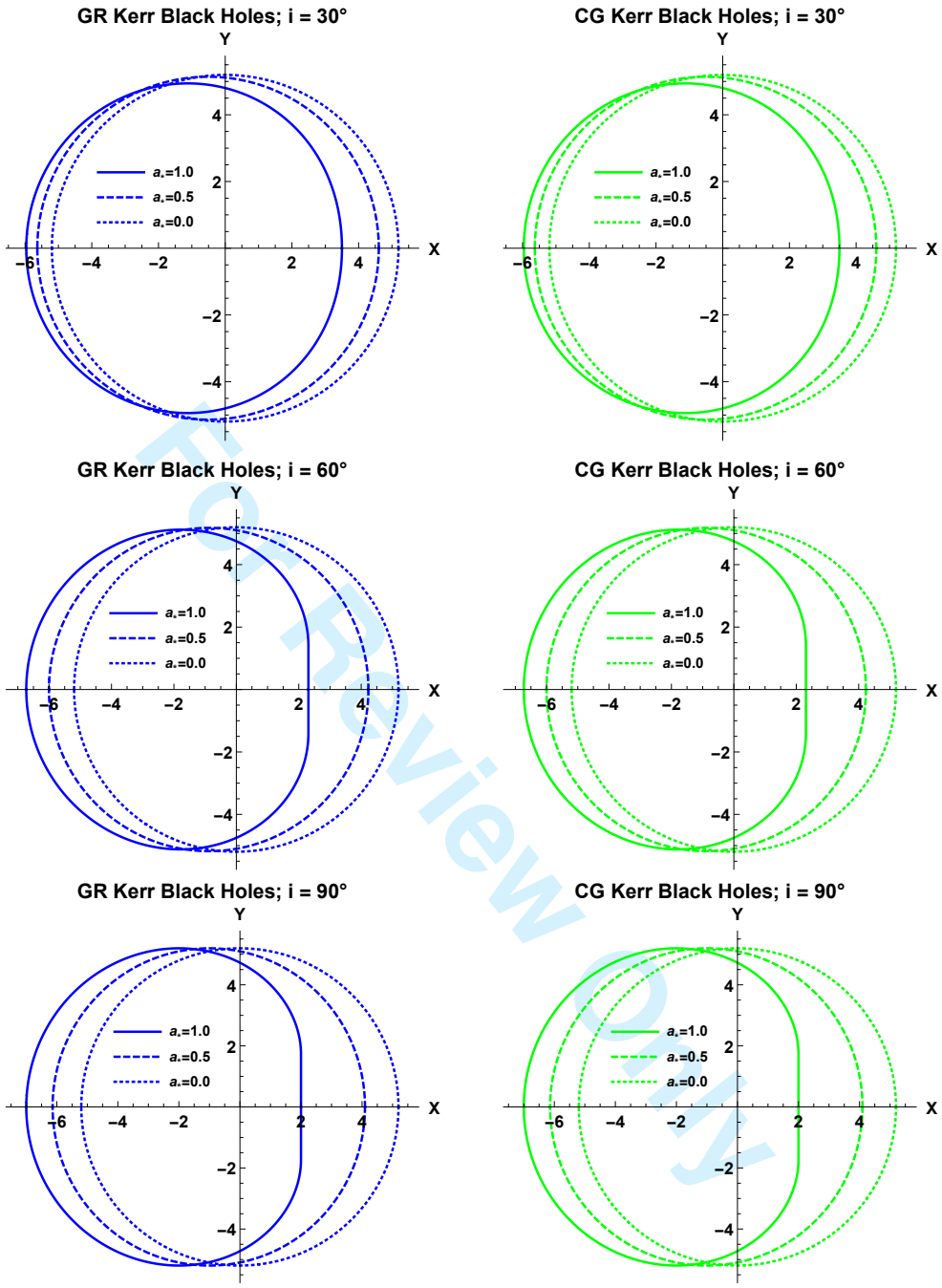

FIG. 1: Kerr black hole shadows, computed following GR and CG, for different values of the angular coordinate i and of the dimensionless parameter a_*. The GR shadows (left panels, in blue) are independent of the black hole mass, while the CG shadows (right panels, in green) are computed using the mass of Sgr A* black hole and the CG parameters from Eq. (5). There are practically no differences between GR and CG plots.

$X_{(CG)}$ and $Y_{(CG)}$ from Eqs. (30)-(31), which depend on the black hole mass through the factor $(1 - \frac{3}{2}\gamma_*) = (1 - \frac{3}{2}M\gamma)$.

The CG shadows also depend critically on the CG parameters γ and κ (or the equivalent γ_* and k_*); for the plots in Fig. 1 we used the values shown in Eq. (5), which represent the largest estimates of these parameters currently in the literature. However, given their small values, no significant differences are noticeable in Fig. 1 between the GR shadows (left panels, in blue) and the CG shadows (right panels, in green). The differences between the GR and CG plots for Sagittarius A* were estimated to be on the order of 10^{-15}, i.e., Kerr black hole shadows computed in CG are virtually the same as those in GR.

Given that EHT observations of the Sgr A* shadow are likely to measure its angular size as $R \simeq (26.4 \pm 1.5)\ \mu$arcsec [8], i.e., with a $\sim 6\%$ uncertainty of the angular radius, no practical differences are expected between GR and CG shadows for Sagittarius A*, due to the extremely small CG corrections ($\sim 10^{-15}$) estimated above.

As our second case, we consider a supermassive black hole with $M \sim 10^{11} M_\odot \sim 10^{16}\,$cm, which correspond to the largest current estimates of black hole masses, such as the S5 0014+813 supermassive BH [70] or similar, and we also increase the values of the CG parameters γ and κ, in order to obtain significant differences between GR and CG shadows.

The CG shadows in the left panels of Fig. 2 (in red) were obtained by using $M = 10^{16}\,$cm, $\gamma = 1.94 \times 10^{-28}\,\text{cm}^{-1}$ (same value for γ as in Eq. (5)), and by increasing the κ parameter by several orders of magnitudes: $\kappa \approx 10^{-34}\,\text{cm}^{-2}$. Similarly, the CG shadows in the right panels of Fig. 2 (in cyan) were obtained by using $M = 10^{16}\,$cm, $\kappa = 6.42 \times 10^{-48}\,\text{cm}^{-2}$ (same value for κ as in Eq. (5)), and by increasing the γ parameter by several orders of magnitudes: $\gamma \approx 10^{-17}\,\text{cm}^{-1}$.

All these CG shadows in Fig. 2 should be compared with the respective GR shadows in Fig. 1 (which are mass independent). The comparison now shows noticeable differences between GR and CG cases. However, the CG plots in Fig. 2 were obtained by using large values of the CG parameters γ and κ, which are currently ruled out by CG analysis of galactic rotation curves and of the cosmological accelerated expansion of the Universe.

Therefore, we conclude that CG Kerr black hole shadows are not likely to look any different from the equivalent GR shadows and thus the Event Horizon Telescope will probably not be able to differentiate between predictions of standard GR and of alternative CG theories.

FIG. 2: Kerr black hole shadows, computed following CG with $M = 10^{16}\,\mathrm{cm}$, for different values of the angular coordinate i and of the dimensionless parameter a_*. The CG shadows in the left panels (in red) are computed with $\kappa \approx 10^{-34}\,\mathrm{cm}^{-2}$, while the CG shadows in the right panels (in cyan) are computed with $\gamma \approx 10^{-17}\,\mathrm{cm}^{-1}$. For these values of the CG parameters there are noticeable differences between CG plots in this Fig. 2 and GR plots from Fig. 1

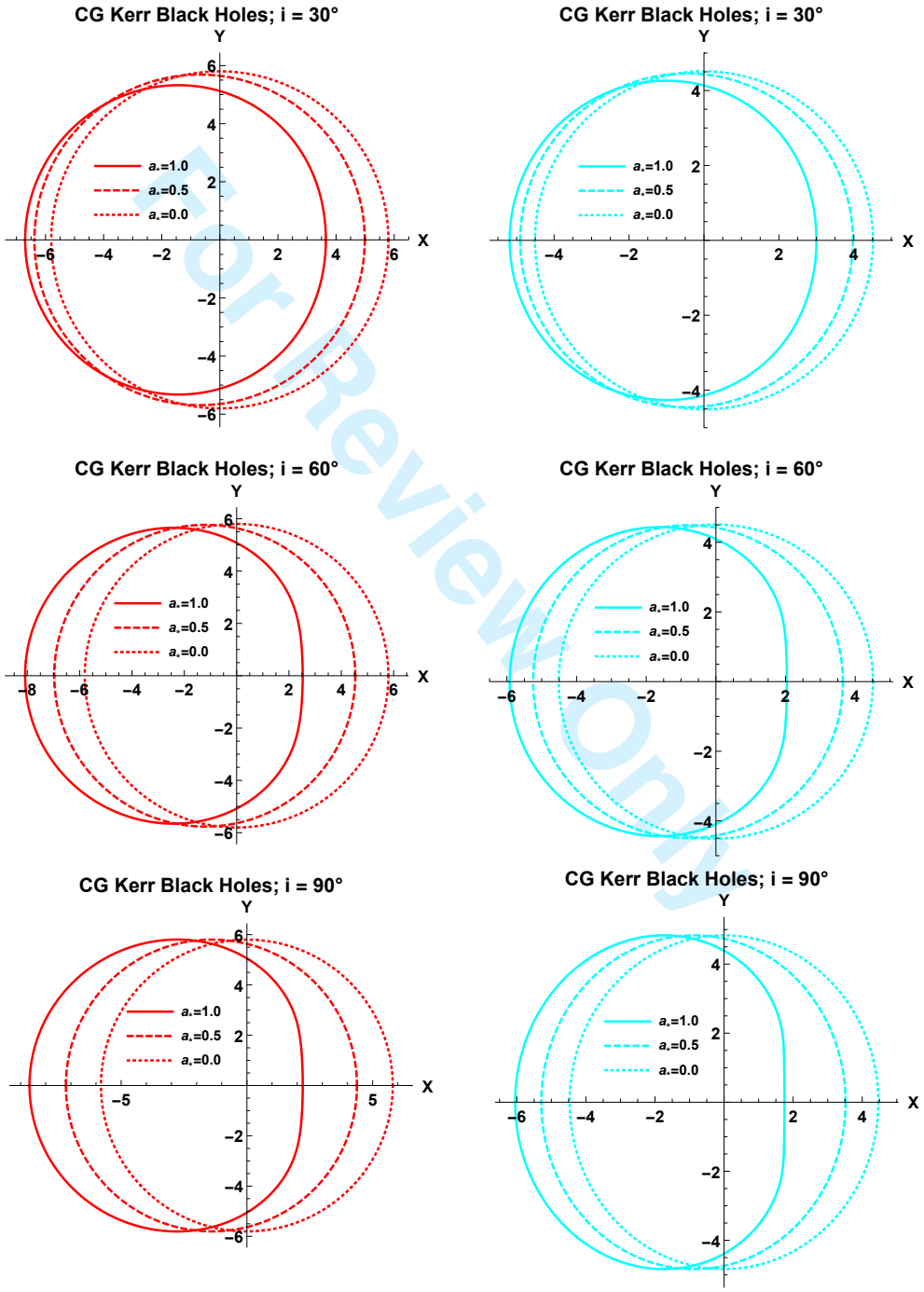

V. CONCLUSIONS

In this paper, we have analyzed the morphology of shadows from a rotating, neutral black hole in a fourth-order conformal Weyl gravity framework, to determine any potentially observable model-dependent characteristics. Since Weyl gravitation provides large-scale modifications to general relativity, the horizon size and mass of Sgr A* should provide a suitable testbed for this theory. Unfortunately, we have shown that the shadow morphology is not affected by the underlying framework, giving a deviation from the GR case on the order of 10^{-15} in the dimensionless coordinates.

A difference measurable by the EHT (*i.e.* greater than 6% of the angular radius) only arises for the largest known supermassive black holes on the order of $M \sim 10^{10} - 10^{11} M_{\odot}$, well above the estimate mass range of Sgr A* ($10^6 M_{\odot}$). In this case, however, the shadow characteristics would be measurably different from those predicted by general relativity if the constraints on the conformal parameters γ and κ are sufficiently loose and increased by several orders of magnitude. This would push the parameters well outside the range provided by experimental observations, however. It is thus unlikely that any differentiable shadow characteristics from pure conformal Weyl gravity will be detected in upcoming experiments.

Since it is anticipated that quantum effects will become realizable on the macroscopic horizon scales of such supermassive BHs, however, one could consider extensions to Weyl CG that include quantum corrections. These might include adding a minimal length scale [71], a non-commutative geometry [72], the Generalized Uncertainty Principle [73], or asymptotic safety [74]. It is possible that such a quantum/cosmological hybrid model could produce the observable effects discussed herein, while bring the CG parameters within their experimentally-constrained range. These quantum effects are currently being investigated by the authors.

[1] B. P. Abbott et al. (Virgo, LIGO Scientific), Phys. Rev. Lett. **116**, 061102 (2016), arXiv:1602.03837 [gr-qc].

[2] B. P. Abbott et al. (Virgo, LIGO Scientific), Phys. Rev. Lett. **116**, 241103 (2016), arXiv:1606.04855 [gr-qc].

[3] B. P. Abbott et al. (Virgo, LIGO Scientific) (2016), arXiv:1606.04856 [gr-qc].

[4] The Event Horizon Telescope Consortium (http://www.eventhorizontelescope.org/).

[5] C. Goddi et al. (2016), arXiv:1606.08879 [astro-ph.HE].

[6] S. Doeleman et al., Nature **455**, 78 (2008), arXiv:0809.2442 [astro-ph].

[7] V. L. Fish, K. Akiyama, K. L. Bouman, A. A. Chael, M. D. Johnson, S. S. Doeleman, L. Blackburn, J. F. C. Wardle, and W. T. Freeman (Event Horizon Telescope) (2016), arXiv:1607.03034 [astro-ph.IM].

[8] T. Johannsen, A. E. Broderick, P. M. Plewa, S. Chatzopoulos, S. S. Doeleman, F. Eisenhauer, V. L. Fish, R. Genzel, O. Gerhard, and M. D. Johnson, Phys. Rev. Lett. **116**, 031101 (2016), arXiv:1512.02640 [astro-ph.GA].

[9] Z. Li and C. Bambi, JCAP **1401**, 041 (2014), arXiv:1309.1606 [gr-qc].

[10] T. Johannsen, Astrophys. J. **777**, 170 (2013), arXiv:1501.02814 [astro-ph.HE].

[11] P. V. P. Cunha, C. A. R. Herdeiro, E. Radu, and H. F. Runarsson, Phys. Rev. Lett. **115**, 211102 (2015), arXiv:1509.00021 [gr-qc].

[12] U. Papnoi, F. Atamurotov, S. G. Ghosh, and B. Ahmedov, Phys. Rev. **D90**, 024073 (2014), arXiv:1407.0834 [gr-qc].

[13] S. Abdolrahimi, R. B. Mann, and C. Tzounis, Phys. Rev. **D91**, 084052 (2015), arXiv:1502.00073 [gr-qc].

[14] S. Abdolrahimi, J. Kunz, P. Nedkova, and C. Tzounis, JCAP **1512**, 009 (2015), arXiv:1509.01665 [gr-qc].

[15] S. Abdolrahimi, R. B. Mann, and C. Tzounis, Phys. Rev. **D92**, 124011 (2015), arXiv:1510.03530 [gr-qc].

[16] S.-W. Wei, P. Cheng, Y. Zhong, and X.-N. Zhou, JCAP **1508**, 004 (2015), arXiv:1501.06298 [gr-qc].

[17] J. W. Moffat, Eur. Phys. J. **C75**, 130 (2015), arXiv:1502.01677 [gr-qc].

[18] S. Dastan, R. Saffari, and S. Soroushfar (2016), arXiv:1606.06994 [gr-qc].

[19] F. Atamurotov, S. G. Ghosh, and B. Ahmedov, Eur. Phys. J. **C76**, 273 (2016), arXiv:1506.03690 [gr-qc].

[20] A. Abdujabbarov, B. Toshmatov, Z. Stuchlk, and B. Ahmedov (2015), arXiv:1512.05206 [gr-qc].

[21] M. Amir and S. G. Ghosh (2016), arXiv:1603.06382 [gr-qc].

[22] S. B. Giddings, Phys. Rev. **D88**, 024018 (2013), arXiv:1302.2613 [hep-th].

[23] S. B. Giddings, Phys. Rev. **D88**, 064023 (2013), arXiv:1211.7070 [hep-th].

[24] S. B. Giddings and Y. Shi, Phys. Rev. **D89**, 124032 (2014), arXiv:1310.5700 [hep-th].

[25] S. B. Giddings, Phys. Rev. **D90**, 124033 (2014), arXiv:1406.7001 [hep-th].

[26] S. B. Giddings and D. Psaltis (2016), arXiv:1606.07814 [astro-ph.HE].

[27] H. Weyl, Math Z. **2**, 384 (1918).

[28] P. D. Mannheim and D. Kazanas, Astrophys. J. **342**, 635 (1989).

[29] D. Kazanas and P. D. Mannheim, Astrophys. J. Suppl. **76**, 431 (1991).

[30] P. D. Mannheim, Prog.Part.Nucl.Phys. **56**, 340 (2006), astro-ph/0505266.

[31] G. U. Varieschi, Gen.Rel.Grav. **42**, 929 (2010), arXiv:0809.4729 [gr-qc].

[32] G. U. Varieschi, ISRN Astron.Astrophys. **2011**, 806549 (2011), arXiv:0812.2472 [astro-ph].

[33] G. U. Varieschi, Gen.Rel.Grav. **46**, 1741 (2014), arXiv:1401.6503 [gr-qc].

[34] G. U. Varieschi, Galaxies **2**, 577 (2014), arXiv:1410.2944 [astro-ph.CO].

[35] G. 't Hooft (2014), arXiv:1410.6675 [gr-qc].

[36] G. 't Hooft (2010), arXiv:1009.0669 [gr-qc].

[37] G. 't Hooft (2010), arXiv:1011.0061 [gr-qc].

[38] G. 't Hooft, Found.Phys. **41** (2011), arXiv:1104.4543 [gr-qc].

[39] P. D. Mannheim, Found. Phys. **42**, 388 (2012), arXiv:1101.2186 [hep-th].

[40] P. D. Mannheim, Gen. Rel. Grav. **22**, 289 (1990).

[41] P. D. Mannheim, Astrophys. J. **561**, 1 (2001), astro-ph/9910093.

[42] P. D. Mannheim, Gen. Rel. Grav. **43**, 703 (2011), arXiv:0909.0212 [hep-th].

[43] P. D. Mannheim and J. G. O'Brien, Phys.Rev. **D85**, 124020 (2012), arXiv:1011.3495 [astro-ph.CO].

[44] J. Maldacena (2011), arXiv:1105.5632 [hep-th].

[45] R. J. Riegert, Phys.Rev.Lett. **53**, 315 (1984).

[46] C. M. Bender and P. D. Mannheim, Phys. Rev. Lett. **100**, 110402 (2008), arXiv:0706.0207 [hep-th].

[47] P. D. Mannheim, in *Proceedings on 13th International Symposium on Particles, strings, and cosmology (PASCOS 2007): London, UK, July 2-7, 2007* (2007), arXiv:0707.2283 [hep-th].

[48] P. D. Mannheim, Found. Phys. **37**, 532 (2007), hep-th/0608154.

[49] C. M. Bender and P. D. Mannheim, Phys. Rev. **D78**, 025022 (2008), arXiv:0804.4190 [hep-th].

[50] P. D. Mannheim and A. Davidson, ArXiv High Energy Physics - Theory e-prints (2000),

hep-th/0001115.

[51] A. Pais and G. E. Uhlenbeck, Phys. Rev. **79**, 145 (1950).

[52] P. D. Mannheim, Phys. Rev. **D75**, 124006 (2007), gr-qc/0703037.

[53] R. Bach, Math Z. **9**, 110 (1921).

[54] P. D. Mannheim, Astrophys. J. **419**, 150 (1993), hep-ph/9212304.

[55] P. D. Mannheim, Astrophys. J. **479**, 659 (1997), astro-ph/9605085.

[56] P. D. Mannheim and J. G. O'Brien, Phys.Rev.Lett. **106**, 121101 (2011), arXiv:1007.0970 [astro-ph.CO].

[57] J. G. O'Brien and P. D. Mannheim, Mon. Not. Roy. Astron. Soc. **421**, 1273 (2012), arXiv:1107.5229 [astro-ph.CO].

[58] P. D. Mannheim and J. G. O'Brien, J. Phys. Conf. Ser. **437**, 012002 (2013), arXiv:1211.0188 [astro-ph.CO].

[59] P. D. Mannheim and D. Kazanas, Gen. Rel. Grav. **26**, 337 (1994).

[60] E. E. Flanagan, Phys. Rev. **D74**, 023002 (2006), astro-ph/0605504.

[61] Y. Yoon, Phys. Rev. **D88**, 027504 (2013), 1305.0163.

[62] P. D. Mannheim, Phys. Rev. **D93**, 068501 (2016), 1506.02479.

[63] S. Chandrasekhar, *The mathematical theory of black holes. New York : Oxford University Press.* (1992).

[64] P. D. Mannheim and D. Kazanas, Phys. Rev. **D44**, 417 (1991).

[65] A. de Vries, Classical and Quantum Gravity **17**, 123 (2000).

[66] S. Gillessen, F. Eisenhauer, S. Trippe, T. Alexander, R. Genzel, F. Martins, and T. Ott, Astrophys. J. **692**, 1075 (2009), arXiv:0810.4674 [astro-ph].

[67] A. M. Ghez et al., Astrophys. J. **689**, 1044 (2008), arXiv:0808.2870 [astro-ph].

[68] A. Boehle, A. M. Ghez, R. Schödel, L. Meyer, S. Yelda, S. Albers, G. D. Martinez, E. E. Becklin, T. Do, J. R. Lu, et al., ArXiv e-prints (2016), arXiv:1607.05726.

[69] F. Eisenhauer, R. Schoedel, R. Genzel, T. Ott, M. Tecza, R. Abuter, A. Eckart, and T. Alexander, Astrophys. J. **597**, L121 (2003), astro-ph/0306220.

[70] G. Ghisellini, L. Foschini, M. Volonteri, G. Ghirlanda, F. Haardt, D. Burlon, and F. Tavecchio, Mon. Not. Roy. Astron. Soc. **399**, L24 (2009), arXiv:0906.0575.

[71] S. Hossenfelder, Living Rev. Rel. **16**, 2 (2013), arXiv:1203.6191 [gr-qc].

[72] P. Nicolini, Int. J. Mod. Phys. **A24**, 1229 (2009), arXiv:0807.1939 [hep-th].

[73] B. J. Carr, J. Mureika, and P. Nicolini, JHEP **07**, 052 (2015), arXiv:1504.07637 [gr-qc].

[74] M. Reuter and J.-M. Schwindt, JHEP **01**, 070 (2006), hep-th/0511021.